Liposome-induced immunosuppression and tumor growth is mediated by macrophages and mitigated by liposome-encapsulated alendronate

Robin Rajan, Manoj K. Sabnani, Vikram Mavinkurve, Hilary Shmeeda, Hossein Mansouri, Sandrine Bonkoungou, Alexander D. Le, Laurence M. Wood, Alberto A. Gabizon, Ninh M. La-Beck

PII: S0168-3659(17)31093-3
DOI: doi:10.1016/j.jconrel.2017.12.023
Reference: COREL 9103

To appear in: *Journal of Controlled Release*

Received date: 21 July 2017
Revised date: 20 December 2017
Accepted date: 21 December 2017

Please cite this article as: Robin Rajan, Manoj K. Sabnani, Vikram Mavinkurve, Hilary Shmeeda, Hossein Mansouri, Sandrine Bonkoungou, Alexander D. Le, Laurence M. Wood, Alberto A. Gabizon, Ninh M. La-Beck , Liposome-induced immunosuppression and tumor growth is mediated by macrophages and mitigated by liposome-encapsulated alendronate. The address for the corresponding author was captured as affiliation for all authors. Please check if appropriate. Corel(2017), doi:10.1016/j.jconrel.2017.12.023

Liposome-induced immunosuppression and tumor growth is mediated by macrophages and mitigated by liposome-encapsulated alendronate

Robin Rajan[a], Manoj K. Sabnani[a,1], Vikram Mavinkurve[a,2], Hilary Shmeeda[b], Hossein Mansouri[c], Sandrine Bonkoungou[a,3], Alexander D. Le[a], Laurence M. Wood[a], Alberto A. Gabizon[b,d], Ninh M. La-Beck[a]

Affiliations:

a. Department of Immunotherapeutics and Biotechnology, Texas Tech University Health Sciences Center School of Pharmacy, Abilene, TX, USA
b. Laboratory of Experimental Oncology, Shaare Zedek Medical Center, Jerusalem, Israel
c. Department of Mathematics and Statistics, Texas Tech University, Lubbock, TX, USA
d. Hebrew University-School of Medicine, Jerusalem, Israel

Running title: Impact of alendronate on liposome-induced immune modulation

Financial support: This work was funded by a National Institutes of Health grant (NCI 1R15CA192097) awarded to NML. Both NML and LMW also received research support from the Development Corporation of Abilene. All authors declare that they have no conflicts of interests.

Parts of this work have been presented at the American Association for Cancer Research 2016 Annual Meeting in New Orleans, LA, and the Mechanisms and Barriers in Nanomedicine Workshop 2016 in Breckenridge, CO.

Correspondence: Ninh M. La-Beck, Pharm.D.
Department of Immunotherapeutics and Biotechnology
Texas Tech University Health Sciences Center School of Pharmacy
1718 Pine St, Abilene, TX 79601
Phone: 325-696-0433
Fax: 325-676-3875
Email: irene.la-beck@ttuhsc.edu

Laurence M. Wood, Ph.D.
Department of Immunotherapeutics and Biotechnology
Texas Tech University Health Sciences Center School of Pharmacy
1718 Pine St, Abilene, TX 79601
Phone: 325-696-0431
Fax: 325-676-3875
Email: Laurence.wood@ttuhsc.edu

Word count: 6543 (body), 267 (abstract); References: 76; Figures: 8; Supplementary materials: 11 Tables, 6 Figures

Footnotes:

1) Current affiliation: Department of Biology, University of Texas at Arlington, Arlington, TX
2) Current affiliation: Memorial-Sloan Kettering Cancer Center, New York, NY
3) Current affiliation: Champions Oncology, Rockville, MD

Abstract

Liposomal nanoparticles are the most commonly used drug nano-delivery platforms. However, recent reports show that certain pegylated liposomal nanoparticles (PLNs) and polymeric nanoparticles have the potential to enhance tumor growth and inhibit antitumor immunity in murine cancer models. We sought herein to identify the mechanisms and determine whether PLN-associated immunosuppression and tumor growth can be reversed using alendronate, an immune modulatory drug. By conducting *in vivo* and *ex vivo* experiments with the immunocompetent TC-1 murine tumor model, we found that macrophages were the primary cells that internalized PLN in the tumor microenvironment and that PLN-induced tumor growth was dependent on macrophages. Treatment with PLN increased immunosuppression as evidenced by increased expression of arginase-1 in $CD11b^{+}Gr1^{+}$ cells, diminished M1 functionality in macrophages, and globally suppressed T-cell cytokine production. Encapsulating alendronate in PLN reversed these effects on myeloid cells and shifted the profile of multi-cytokine producing T-cells towards an $IFN\gamma^{+}$ $perforin^{+}$ response, suggesting increased cytotoxic functionality. Importantly, we also found that PLN-encapsulated alendronate (PLN-alen), but not free alendronate, abrogated PLN-induced tumor growth and increased progression-free survival. In summary, we have identified a novel mechanism of PLN-induced tumor growth through macrophage polarization and immunosuppression that can be targeted and inactivated to improve the anticancer efficacy of PLN-delivered drugs. Importantly, we also determined that PLN-alen not only reversed protumoral effects of the PLN carrier, but also had moderate antitumor activity. Our findings strongly support the inclusion of immune-responsive tumor models and in-depth immune functional studies in the preclinical drug development paradigm for cancer nanomedicines, and the further development of chemo-immunotherapy strategies to co-deliver alendronate and chemotherapy for the treatment of cancer.

Key words: nanoparticle, liposome, immune modulation, alendronate, cancer immunology

1.0 Introduction

Nanoparticle-based drugs are a heterogeneous class of pharmaceuticals, also referred as nanomedicines, characterized by the co-formulation of one or more active drug entities with a carrier system [1, 2]. The resulting nanomedicines are within the nanometer scale, usually in the range of 10 to 200 nm in diameter. Nanoparticles are used as drug carriers for cancer therapies since they have pharmacological advantages such as increased tumor drug delivery through the enhanced permeability and retention (EPR) effect, protection of the drug cargo from degradation, and in most cases improved tolerability of cytotoxic drugs [3-5]. There are now nine nanoparticle drugs approved for the treatment of cancer (Supplemental Table S1), and most utilize liposomal nanoparticles because the lipid components are considered biocompatible and safe materials and liposomes have been manufactured in bulk and met regulatory criteria. However, many liposomal drugs and other nanoparticle-based drug formulations have failed to meet regulatory criteria for approval or have shown only modest anticancer efficacy in phase 3 clinical studies [6-11]. A recent meta-analysis of 14 randomized clinical trials that directly compared the anticancer efficacy of liposomal formulations of cytotoxic chemotherapy to their conventional “free” drug formulation found that liposome encapsulation of drugs did not improve objective response rates, progression-free survival, or overall survival in patients with solid tumors [9]. Currently the only liposomal drug to significantly prolong cancer patient survival in a head-to-head trial with the equivalent conventional formulation is CPX-351 (Vyxeos; liposomal daunarubicin and cytarabine). This was achieved via co-delivery of two cytotoxic drugs in patients with acute myelogenous leukemia [12] where the EPR effect would not be expected to play a role. This implies that there are critical knowledge gaps in the current understanding of the pharmacology of liposomal drugs in the treatment of cancer that need to be addressed in order to make major advances in the field.

Although the reasons for the lack of translation between preclinical anticancer efficacy and clinical findings are not fully understood, it is likely that the immune system is a key player since nanoparticles are known to activate or inhibit components of the immune system. The tumor microenvironment is infiltrated by a multitude of antitumor effector immune cells and immunosuppressive cells recruited by the tumor. Tumor evasion of $CD8^+$ T-cell cytolytic activity is associated with disease progression [13] and there are several mechanisms by which the tumor evades $CD8^+$ T-cell mediated destruction such as downregulation of MHC Class I and mutation of antigenic proteins [14]. While liposomes are unlikely to manipulate the mechanisms involved in immune-mediated recognition of tumors, there is evidence suggesting they contribute to the recruitment or induction of immunosuppressive cell types into the tumor microenvironment [15]. Myeloid-derived suppressor cells (MDSCs), that highly express arginase-1 and produce anti-inflammatory cytokines infiltrate tumors and secondary lymphoid organs in tumor-bearing mice and inhibit T-cell antitumor responses and enhance tumor angiogenesis leading to tumor progression [16, 17]. Beyond MDSCs, other myeloid cells such as tumor-associated macrophage (TAMs) also regulate antitumor immunity. While classically activated inflammatory macrophage, known as M1 macrophage, can inhibit tumor growth through inducible nitric oxide synthase (iNOS)-mediated production of reactive nitrogen species (RNS), many TAMs are instead polarized as alternatively activated anti-inflammatory M2 macrophage. M2 macrophages do not express iNOS but have elevated expression of arginase that prevents nitric oxide production, and secrete anti-inflammatory cytokines such as IL-10 and TGFβ.

The clinical implications of interactions between nanomedicines and the immune system have been previously reviewed in detail [18]. Briefly, these interactions with the immune system can affect drug tolerability, immunogenicity, and pharmacokinetics in patients. However, their impact on tumors is only

beginning to be elucidated. It was reported that polystyrene nanoparticles enhanced tumor growth in murine cancer models through mechanisms involving complement C5a receptors and MDSCs, suggesting that interactions between nanoparticles and the immune system can have protumoral effects [19]. In addition, we have previously reported that a poly-ethylene glycol (PEG)-coated (pegylated) liposomal nanoparticle (PLN) carrier, similar to that used in patients, significantly enhanced tumor growth in mice bearing TC-1 tumors, a mouse model of human papilloma virus (HPV)-induced cancer [20]. In these studies, PLNs were administered as weekly intravenous injections at clinically relevant lipid doses (four doses of 47 nmoles/g or two doses of 85 nmoles/g). Treatment with PLN was associated with suppression of antitumor immunity as indicated by decreased interferon-γ (IFNγ) production by tumor-associated macrophages (TAMs) and cytotoxic T-cells, diminished tumor infiltration of HPV E7-tumor antigen-specific T-cells, and decreased number of dendritic cells in tumor draining lymph nodes. These data suggest that PLN-induced immunosuppression and tumor enhancement may mitigate the benefits of carrier-mediated drug delivery (Figure 1) and could partially explain why there is often an insufficient improvement in the clinical efficacy of liposomal drugs over free drugs [7, 8, 10, 21]. The mechanisms underlying the observed PLN-associated tumor promotion are currently not known but it is likely that immunosuppressive cells such as TAMs are mediators since they have been implicated as players in both the pharmacology of liposome-mediated therapies [22, 23] and in cancer progression [17, 24]. In theory, the tumor promoting effects of the PLN may diminish the antitumor effects of the drug cargo. However, it is also possible that cytotoxic cargo may kill not only tumor cells but also immune cells responsible for the tumor promoting effects of the carrier, thus mitigating the PLN impact on cancer progression.

Figure 1. A proposed model of how interactions between the nanoparticle carrier, drug cargo, and immune system impact overall therapeutic efficacy of nanoparticle-delivered drugs. EPR, enhanced permeability and retention effect; MPS, mononuclear phagocyte system

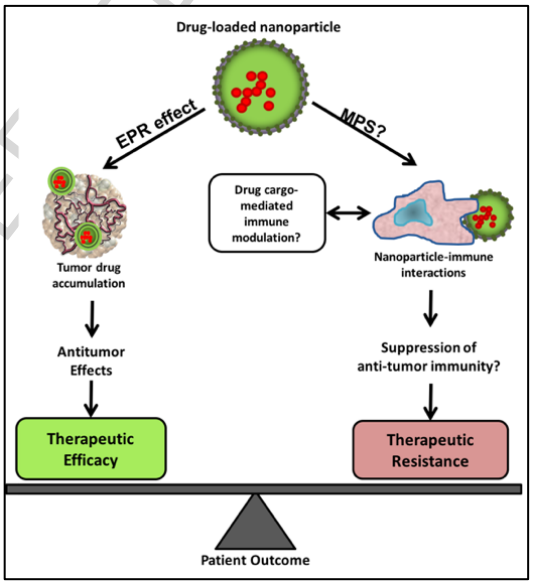

The imperative question that must be answered then is how the drug cargo alters the tumor-promoting and immune modulatory effects of the carrier. Nanoparticles are increasingly used as carriers for targeted therapies and immunotherapies that have significantly less direct cytotoxic effects on immune cells than traditional chemotherapy. In this scenario, the interactions between the carrier and the immune system can be of paramount importance to the overall anticancer efficacy of the carrier-

mediated drug. The primary purpose of this study was to identify the subpopulation of immune cells which mediate the tumor promoting effects of particulate carrier systems, and to determine whether the tumor promoting and immunosuppressive effects of the carrier can be reversed with an immune modulatory and non-cytotoxic drug cargo. We chose PLN as the model carrier since we previously observed enhanced tumor growth with this nanoparticle [20]. We chose alendronate, an aminobisphosphonate, as the model drug cargo because PLN-encapsulated alendronate (PLN-alen) is not cytotoxic to leukocytes [25] and our formulation did not deplete tissue macrophages (Supplemental Figure S1). Moreover, alendronate has been found to have antitumor activity through its effects on T-cells [26] which we theorized would mitigate the immunosuppressive effects of the PLN carrier.

2.0 Materials and Methods

2.1 Cells

TC-1 tumorigenic cells were cultured under standard conditions similar to previously described methods [27]. TC-1 cells are derived from primary epithelial cells of C57BL/6 mice that have been co-transformed with HPV-16 E6 and E7 and c-Ha-ras oncogenes. TC-1 is an established tumor model utilized for the development of cancer immunotherapy since it is responsive to immune modulation and is characterized by immune cell infiltrates [28].

2.2 Formulations

Placebo (i.e., no drug loaded within) PLN similar in size and composition to the Doxil® (pegylated liposomal doxorubicin; PLD) drug carrier, were synthesized using standard extrusion methods as previously described [29]. The PLNs were unilamellar and composed of hydrogenated phosphatidylcholine, cholesterol, and methoxy-polyethylene glycol-distearoyl phosphatidylethanolamine at a molar ratio of 55:40:5, respectively, with an average diameter of 80 nm and poly dispersity index (PDI) $\leq$0.10 as determined by dynamic light scattering. Similar PLNs were also loaded with ammonium alendronate (PLN-alen) at the maximum loadable concentration, 4 to 5 mg/ml, depending on the batch. Unencapsulated alendronate was removed by dialysis along with anion exchange resin chromatography, as described previously [25, 30]. The PLN-alen particles were typically 70-90 nm in mean diameter with PDI approximately 0.05. The alendronate concentration was verified post synthesis and drug release profiles in buffer and plasma determined as previously detailed [30]. In buffer, PLN-alen is very stable with negligible leakage of alendronate for at least 1 year storage at 4°C. In plasma, it is also very stable for several hours incubation at 37°C. All formulations were endotoxin-free and sterile.

2.3 Animals and treatments

Six to twelve weeks old male and female wildtype C57BL/6 mice (Jackson Laboratories, Bar Harbor, ME), macrophage FAS-induced apoptosis (MaFIA) transgenic mice on C57BL/6 background (Jackson Laboratories), and OT1 transgenic mice on C57BL/6 background (Jackson Laboratories) were housed and cared for at the Texas Tech University Health Sciences Center (TTUHSC) animal care facility (Abilene, Texas) according to the Institutional Animal Care and Use Committee guidelines and all procedures were conducted under an approved protocol. To evaluate the effect on tumors, 0.5×10^6 TC-1 tumorigenic cells were implanted subcutaneously on the hind flank and tumor volume was monitored at least twice weekly using digital calipers. Tumor volume was estimated using the formula Volume = $A*B^2/2$, where A = largest diameter and B = smaller diameter.

To identify the cell types which internalized intravenously administered PLN, wildtype mice (n=8 total) bearing TC-1 implanted tumors were randomized to be treated with fluorescent nitrobenzoxadiazole (NBD)-labelled PLN or vehicle control. The mice were sacrificed 48 hours later, tumors were resected and enzymatically processed to obtain single cell suspensions which were then stained with antibodies against CD45, CD11b, F4/80 and Gr-1, and liposome uptake by different cell populations was visualized using imaging flow cytometry (ImageStreamX, EMD Millipore) and quantified using conventional flow cytometry (BD LSR Fortessa) (details are in supplemental materials).

MaFIA mice (n=24 total) were used to determine the role of macrophages in PLN-induced tumor growth. In MaFIA mice, colony stimulating factor receptor 1 (Csf1r) drives expression of FK506 binding protein 1A (Fas), an inducible "suicide" gene. Since Csf1r is expressed in macrophages and not lymphocytes, this allows selective elimination of up to 90% of systemic macrophages after administration of the Fas receptor ligand, AP20187 (Clontech) [31]. Depletion of macrophages was achieved by intraperitoneal administration of AP20187 as described previously [31]. Mice were randomized to receive AP20187 or vehicle control (4% ethanol, 1% PEG, 1.7% Tween in water) and mice in each group were further randomized to receive PLN at 85 nmoles of phospholipids per gram body weight or equivalent volume of the vehicle (5% dextrose solution) administered via tail vein injections for two weekly doses.

To assess the impact of PLN and PLN-alen on immune functionality, wildtype mice (n=12) were randomly allocated into treatment groups to receive PLN at 85 nmoles of phospholipids per gram body weight, PLN-alen at equivalent phospholipid concentration (alendronate at 7 μg/g), or equivalent volume of vehicle (5% dextrose solution) via tail vein injections. Animals were sacrificed 7 days later for collection of splenocytes since prior experiments indicated that this was the time when PLN-alen induced effects on splenocytes peaked. The alendronate dose is compatible with the maximum tolerated dose of PLN-alen determined in prior experiments (unpublished).

To determine the impact on tumor growth, mice (n=28) were subcutaneously implanted with 0.5 x 10^6 TC-1 tumorigenic cells on the hind flank and randomized 72 hours later to receive PLN, PLN-alen, PLN + free alendronate (at equivalent phospholipid and alendronate concentrations), or equivalent volume of vehicle control (5% dextrose solution) via tail vein injections as described above. Tumor size was measured twice weekly with digital calipers. To evaluate the acute changes in tumor immune cell infiltration, mice bearing TC-1 tumors (n=24) were sacrificed 48 hours after dosing with PLN, PLN-alen, or vehicle and tumor tissue collected for analysis since this is the time of peak PLN-alen accumulation in tumor tissue [30].

2.4 Cell isolation and tissue processing

Spleens and tumors were excised and processed to obtain single cell suspensions as previously described [20]. Briefly, spleens were dissociated and passed through a 40 μm cell strainer, and red blood cells were lysed with ACK solution (K.D Medical, Columbia, Maryland). Tumors were minced then enzymatically digested and further purified using 30% Percoll density gradient. Single cell suspensions were counted and viability assessed using trypan blue exclusion assay (Vi-Cell XR, Beckman Coulter Inc. California, USA). Cells were then aliquoted out for staining and flow cytometric analyses, or *ex vivo* functional studies as detailed below. In some experiments, tumor tissue was immediately stored in RNALater at -20°C. RNA-stabilized tumor tissue was subsequently processed with the RNeasy RNA extraction kit (Qiagen) in order to obtain total RNA (500 ng) that was then converted to cDNA using the High Capacity Reverse Transcriptase Kit (Thermo Fisher/Applied Biosystems). The cDNA was

analysed by quantitative polymerase chain reaction (qPCR) using a StepOnePlus Real Time PCR System (Thermo Fisher) with primers specific for iNOS, TNFα, IFNγ, and expression was normalized to 18S rRNA.

2.5 Immunophenotyping

Two million cells from each sample were stained for CD45 and myeloid cell markers (CD11b, Gr1, F4/80, CD11c) or T-cell markers (TCR-β, CD8b, CD4). After surface staining, cells in the myeloid panel were fixed, permeabilized, and stained for expression of iNOS and arginase-1 (Arg1). Details of the staining panel are in supplemental materials (Supplemental Tables S2 and S3). Samples were analyzed with a BDLSR Fortessa flow cytometer (BD Biosciences, San Jose, CA) and results analyzed using FlowJo software (Tree Star Inc., Ashland, Oregon, USA). One million events were acquired and single cells were gated using the forward scatter and side scatter parameters, followed by dead cell exclusion via a fixable viability dye (eBioscience, cat. 65-0866-14). Splenic myeloid cells (macrophages, resident monocytes, inflammatory monocytes, granulocytes, and dendritic cells) and tumor myeloid cells (TAM and MDSC) were identified and enumerated. Expression of iNOS and Arg1 was used to define M1 ($iNOS^+Arg1^-$), M2 ($iNOS^-Arg1^+$), and mixed M1/M2 ($iNOS^+Arg1^+$) phenotypes [32, 33]. T-cells ($TCR\beta^+CD8b^+$ or $TCR\beta^+CD4^+$) were enumerated in a similar manner. Details of the gating strategy are in supplemental materials (Supplemental Figure S2).

2.6 *Ex vivo* functional studies

In some experiments, an aliquot of each single cell suspension was also used for evaluation of *ex vivo* T-cell cytokine production studies. Myeloid cells expressing CD11b were removed using a magnetic bead-based assay (Dynabeads FlowComp Flexi kit, ThermoFisher Scientific) according to the product instructions. The remaining splenocytes were stimulated in complete RPMI media with 10% FBS, with cell activation cocktail containing PMA:Ionomycin:Brefeldin A (0.08uM:1.3uM:5 ug/ml) (Biolegend, San Diego, CA) at 37°C for 6 hrs in order to activate intracellular signaling cascades that mimic activation through T-cell receptor, then stained for intracellular cytokines (IFNγ, TNFα, IL-2) and perforin. Samples were analyzed similar to the method described above (staining panels are in supplemental materials).

2.7 Statistical analysis

Statistical analyses were performed using SAS software (version 9.4, SAS Institute Inc., Cary, NC), and all data are expressed as mean + standard error of the mean (SEM), unless otherwise specified. For longitudinal observations of tumor growth, a two-factor (time vs. treatments) repeated measures model with interaction between time and the treatments was considered and tumor volume at endpoint were compared using the Holm-Tukey simultaneous multiple comparisons of the treatment effects in order to control the familywise (overall) Type I error rate. To compare two treatments based on small sample sizes, the exact Wilcoxon rank-sum test was used for each comparison since this method produces the most reliable analysis for small data sets. If data sets involving pairwise comparisons of more than two treatments were observed to be heteroscedastic, rank transformation was used to alleviate heteroscedasticity and then simultaneous pairwise comparisons of treatment effects were conducted based on the rank-transformed data for the one-way analysis of variance model [34, 35]. For analysis of progression-free survival, tumor-free survival was defined as a tumor volume <100 mm^3, and Kaplan-Meier survival curves were used to compare across treatment groups using the Log-Rank test. Tumor growth to >100 mm^3 volume was considered a tumor progression event. An adjusted *P*-value (the

smallest familywise error rate at which the hypothesis can be rejected) of less than 0.05 was considered statistically significant.

3.0 Results

3.1 Macrophages mediate protumoral effects of pegylated liposomes

It was recently reported that PLN significantly enhanced tumor growth in a murine model of cancer and this was associated with diminished T-cell functionality and tumor infiltration [20], suggesting inhibition of antitumor immunity. We theorized that mechanisms of PLN-induced tumor growth involve immunosuppressive leukocytes such as tumor-associated macrophages (TAM) since macrophages have been implicated as key players in both the pharmacology of carrier-mediated therapies [22, 23] and in cancer progression [17, 24]. To test this hypothesis, we first sought to identify the cells within tumor tissue that engulf systemically administered PLN. We found that there was significant internalization of PLN by TAM and $CD11b^{+}Gr1^{+}$ myeloid progenitor cells ($P = 0.029$) but not by tumor-infiltrating lymphocytes (Figure 2A-C) or non-leukocytes (data not shown), suggesting that macrophages mediating protumoral effects of PLN. To verify this, we next conducted tumor growth studies in MaFIA mice treated with PLN or vehicle control, with and without *in vivo* macrophage depletion. We found that depletion of macrophages abrogated PLN-induced tumor growth (Figure 2D; $P < 0.0001$), indicating that they are the primary mediators of the protumoral effects of the carrier.

Figure 2. PLN-induced tumor growth is mediated by macrophages. (A-C) PLNs are internalized by macrophages and $CD11b^{+}Gr1^{+}$ cells in the tumor microenvironment but not by other leukocytes. Mice (n= 8 total) bearing TC-1 tumors were treated intravenously with fluorescent NBD-labelled PLN (NBD-PLN) or vehicle control, tumors were harvested 24 hours later and dissociated to obtain cells for FACS analysis. Representative images of macrophages ($CD11b^{+}F4/80^{+}$) (A) with and (B) without internalized NBD-PLN. (C) NBD fluorescence was determined in each cell population. (D) *In vivo* depletion of systemic macrophages abolished PLN-induced tumor growth. MaFIA transgenic mice (n= 24 total) bearing TC-1 tumors were treated with PLN or vehicle control, with macrophage depletion (AP20187) or mock depletion (vehicle). Data are mean+SEM, *P*-value based on (C) Wilcoxon two-sample rank-sum test, and (D) Holm-Tukey simultaneous multiple comparisons for two-factor analysis of variance with repeated measures; n.s., not significant.

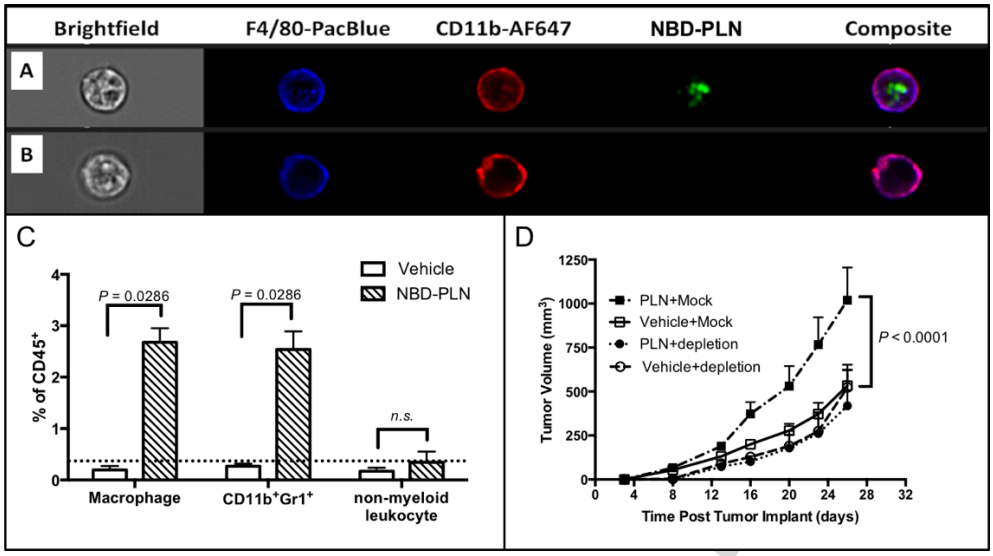

3.2 PLN-alendronate mitigates carrier-induced splenic myeloid cell infiltration and polarization

Given that PLNs are increasingly used as carriers for targeted therapies and immunotherapies, we aimed to determine whether the tumor promoting effects of the carrier can be reversed with an immune modulatory and non-cytotoxic drug cargo. Since alendronate inhibits the activity of osteoclasts, a specialized population of bone macrophages and has been found to have antitumor activity through its effects on T-cells [26], we theorize that formulating PLN with alendronate will mitigate the immunosuppressive effects of the carrier that are mediated by macrophages. To test this strategy, we treated tumor-bearing mice with PLN-alen, PLN, or vehicle control and determined the impact on splenocytes. We chose to inspect splenocytes, (consisting of myeloid and lymphoid immune cells including macrophages, MDSCs, and T cells) because the spleen is a secondary lymphoid organ and this collection of splenic cells plays an important role in the immune response to cancer [36]. Paradoxically, the spleen may even serve as site that helps orchestrate tumor immune tolerance [37]. We found that PLN significantly increased the splenic population of $CD11b^{+}Gr1^{+}$ cells as compared to vehicle control ($P = 0.021$) (Figure 3A-B). In contrast, PLN-alen resulted in a reduction of the splenic population of $CD11b^{+}Gr1^{+}$ cells compared to PLN, and did not result in significant accumulation in comparison to vehicle control (Figure 3A-B). Since the splenic $CD11b^{+}Gr1^{+}$ cell population consists of numerous subpopulations of granulocytic and monocytic cells with the potential to impede T-cell mediated immunity during cancer and infection [38-40], we further characterized the splenic $CD11b^{+}Gr1^{+}$ cell subpopulations in each treatment group. This revealed significant accumulation of granulocytes, consisting of neutrophils, basophils and eosinophils in the PLN treated group ($P = 0.034$) that was not observed with PLN-alen (Figure 3C). Moreover, significant accumulation of both inflammatory and resident monocytes was also observed after PLN treatment ($P = 0.021$ and $P = 0.040$, respectively) but not with PLN-alen (Figure 3C), suggesting that loading alendronate mitigated these effects of the PLN.

Figure 3. PLN-associated accumulation of splenic macrophages, monocytes, and granulocytes is mitigated by the alendronate cargo. Mice were treated with PLN, PLN-alen, or vehicle control and splenocytes were harvested 7 days post dose for immunophenotyping. (A-B) PLN increase splenic accumulation of CD11b+ Gr1+ cells while PLN-alen did not. (C)The $CD11b^{+}Gr1^{+}$ subpopulations that increased were inflammatory monocytes and granulocytes, but an increase in resident monocytes was

also observed. Total n = 11; data are mean+SEM (rank-transformed data in Supplemental Tables S4-S9); one-way analysis of variance based on ranks; n.s., not significant.

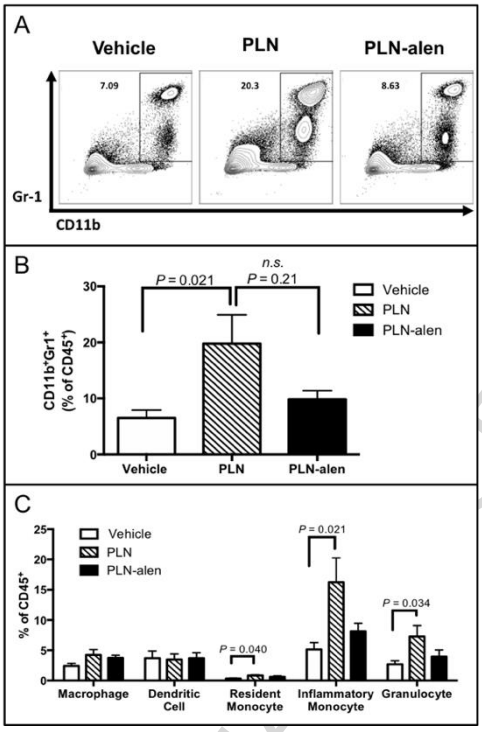

In addition to these effects on splenic myeloid cell accumulation, we observed that PLN increased expression of arginase-1 in $CD11b^{+}Gr^{+}$ cells as compared to vehicle control ($P = 0.032$), suggesting immunosuppressive functionality in this population, whereas PLN-alen did not (Figure 4A). Moreover, splenic macrophages were predominantly M1-like in control mice while PLN treatment diminished M1-macrophages ($P = 0.034$) and increased M2-macrophages, and PLN-alen moderately alleviated this effect of the carrier on M2-macrophages (Figure 4B).

Figure 4. PLN-associated polarization of splenic macrophages and immature myeloid cells towards an M2-like phenotype is differentially affected by the alendronate cargo. (A) PLN treatment increased arginase-1 in the non-macrophage $CD11b^{+}Gr1^{+}$ cells although this effect was reversed when alendronate was loaded into the carrier. (B) Intracellular iNOS and arginase-1 expression was used to define M1 (iNOS+ arg1-), M2 (iNOS- arg1+), and mixed M1/M2 (iNOS+ arg1+) phenotypes in macrophages. Both PLN and PLN-alen increased M2 macrophages and decreased M1 macrophages. Total n = 11; data are mean+SEM (rank-transformed data in Supplemental Table S10); (A) one-way analysis of variance based on ranks and (B) multiple comparisons based on observations.

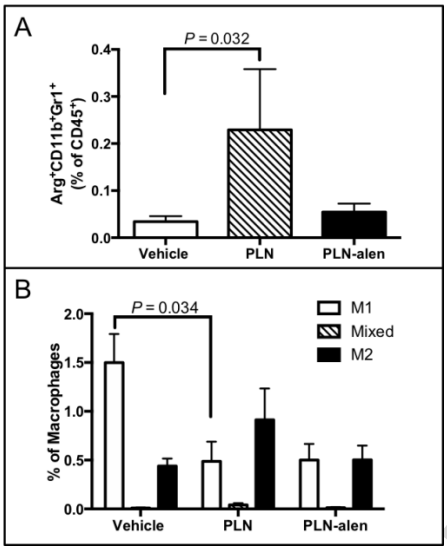

To further probe the impact of treatment on immune functionality, we assessed T-cell cytokine and perforin production in response to *ex vivo* stimulation with PMA/ionomycin. We observed that both PLN and PLN-alen diminished overall cytokine production in $CD8^+$ T-cells (Figure 5), consistent with an immunomodulatory effect by the PLN carrier and its drug cargo. Interestingly, loading alendronate into PLN resulted in a shift in the profile of multi-cytokine producing T-cells, with increased proportions of $IFN\gamma^+perforin^+$ multi-cytokine producing $CD8^+$ T-cells (Supplemental Figure S4), suggesting increased cytolytic potential. Taken together, these immunological changes indicate that the PLN carrier may increase accumulation of myeloid cells with immunosuppressive functionality and globally suppress $CD8^+$ T-cell cytokine production. Loading alendronate into PLN appeared to alleviate the effects of the carrier on myeloid cell accumulation and functional polarization, with moderate potentiation of T-cell $IFN\gamma^+perforin^+$ responses.

Figure 5. PLN inhibit global cytokine production in $CD8^+$ T-cells. Both PLN and PLN-alen inhibited global cytokine production in $CD8^+$ T-cells. Cytokine production was determined by *ex vivo* stimulation with PMA/ionomycin in the presence of brefeldin A and analyzed by FACS. Total n = 10; data are group means.

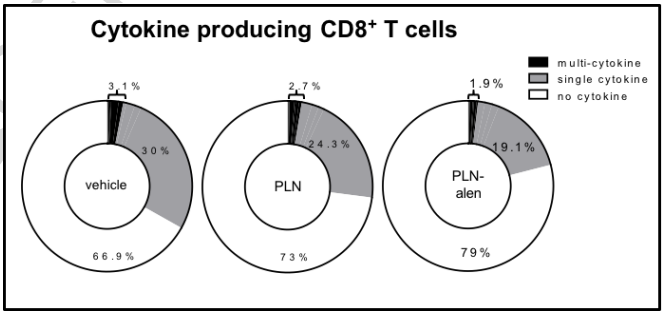

3.3 PLN-alendronate abrogates carrier-induced tumor growth

We next determined the extent to which loading alendronate into PLN would abolish the tumor promoting effects previously reported to be associated with the PLN carrier. We found that PLN significantly accelerated tumor progression compared to vehicle control; the mean tumor volumes at endpoint were 886 mm^3 and 374 mm^3, respectively ($P < 0.0001$) (Figure 6A) and tumor-free survival was significantly diminished in PLN treated mice ($P = 0.0046$) (Figure 6B). Importantly PLN-alen not only abolished this effect but also appeared to have moderate antitumor effects with mean tumor

volume in PLN-alen treated mice of 289 mm^3 (Figure 6A) and significantly longer tumor-free survival compared to vehicle treated mice (P = 0.028) (Figure 6B). This appeared to require carrier-mediated delivery of alendronate since co-administration of PLN with conventional "free" alendronate only minimally diminished the tumor-promoting potential of the lipid carrier (Figure 6A).

Figure 6. PLN-associated tumor progression is abolished by encapsulated alendronate but not free alendronate. Mice implanted with TC-1 tumorigenic cells were treated intravenously with PLN, PLN + free alendronate (PLN + alen), PLN-alen, or vehicle control. Data are from two independent experiments (total n=28), (A) tumor volumes are expressed as mean+SEM; Holm-Tukey simultaneous multiple comparisons for two-factor analysis of variance with repeated measures, and (B) Kaplan-Meier survival curves of time to tumor growth to >100 mm^3 volume with Log-Rank test comparing the groups.

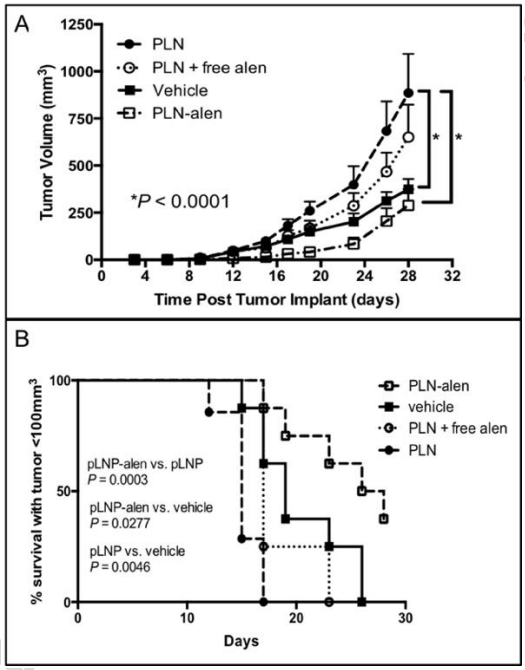

3.4 PLN-alen diminished carrier-induced tumor immunosuppression

We examined the tumor-associated leukocyte populations since prior reports suggest that PLN may alter TAM functionality. Similar to previously published findings [20], we also observed that PLN increased the number of TAMs, and this effect was prevented by PLN-alen, although these findings did not reach statistical significance probably due to the small sample size (Supplemental Figure S5). To determine the impact on activation and polarization of TAMs, expression of iNOS (typical of classically activated inflammatory M1 macrophages) and Arg1 (typical of alternatively-activated anti-inflammatory M2 macrophages) [32, 33], were assessed by flow cytometry. We found that PLN, but not PLN-alen, increased numbers of a mixed M1/M2 TAM population, characterized by production of both iNOS and Arg1, as compared to vehicle control (P = 0.045) (Figure 7A). In addition to TAMs, $CD11b^+Gr1^+$ myeloid cells have also been shown to play a role in promoting cancer progression. While not statistically significant, we observed that PLN increased Arg1 expression in MDSC, whereas PLN-alen diminished this effect of the carrier (Figure 7B). Together, these results indicate that PLN enhances immunosuppressive potential of myeloid cells in the tumor microenvironment and suggest that encapsulating alendronate counteracts these effects. Further, tumor gene expression analysis of M1

macrophage marker (iNOS) and cytokines (TNFα and IFNγ) supports these flow cytometry data (Supplemental Figure S6). Vehicle-treated and PLN-treated mice had low tumor-associated expression of iNOS suggesting a tolerogenic TAM profile. However, co-administration of alendronate, either free or encapsulated, along with PLN resulted in elevated expression of iNOS within the tumor. These data suggest that alendronate may induce skewing of the TAM phenotype from M2 to M1 or mixed M1/M2 phenotypes. In addition, PLN suppressed IFNγ and TNFα gene expression in tumors, consistent with previously published findings supporting an immunosuppressed state.

Figure 7. PLN-alen mitigates carrier-associated effects on tumor-associated leukocytes. Mice bearing implanted TC-1 tumors were treated intravenously with PLN, PLN-alen, free alendronate (alen), or vehicle and sacrificed 48 hrs later to obtain tumor-derived single cell suspensions for immunophenotyping. Intracellular inducible nitric oxide synthase (iNOS) and arginase-1 (Arg1) expression was used to define M1 ($iNOS^+Arg1^-$), M2 ($iNOS^-Arg1^+$), and mixed M1/M2 ($iNOS^+Arg1^+$) TAMs; unactivated ($iNOS^-Arg1^-$) are not shown. (A) PLN polarized TAMs towards a mixed M1/M2 phenotype, whereas this was abolished by PLN-alen. (B) PLN, but not PLN-alen, increased Arg1 expression in myeloid-derived suppressor cells (MDSC). Total n=24, expressed as mean+SEM (rank-transformed data in Supplemental Table S11); one-way analysis of variance based on ranks for vehicle, PLN, and PLN-alen.

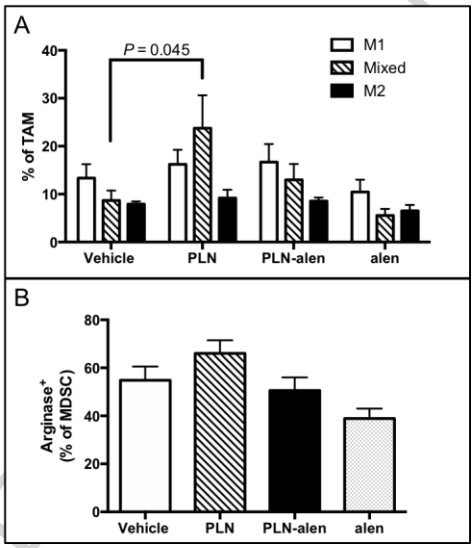

4.0 Discussion

Drug delivery using nanoparticle carriers drastically alters the pharmacokinetics and pharmacodynamics of the drug cargo as compared to the conventional non-carrier mediated formulation due to changes in tissue and cellular distribution dictated by the carrier [41]. This has been exploited to improve drug pharmacokinetic parameters (e.g., half-life, clearance, systemic exposure), enable passive tumor targeting through the EPR effect and active targeting through functionalization with targeting moieties such as antibodies, and to considerably improve tolerability by limiting normal tissue exposure. However, carrier-mediated formulations also significantly increase interactions with the immune system and these interactions have the potential to lead to detrimental effects [18, 42].

In patients, the acute infusion reactions associated with administration of liposomal drugs has been linked to carrier-induced complement activation [43, 44] and production of complement anaphylotoxins C3a, C4a, and C5a [45]. Nanoparticles are also internalized by cells of the MPS such as hepatic Kupffer cells and splenic macrophages [46, 47]. This interaction with the MPS may have important

clinical significance as low MPS function or cell count has been shown to correlate with decreased nanoparticle clearance in patients and in several preclinical animal models [22, 23]. Although carrier interactions with the immune system have been shown to affect drug pharmacokinetics and toxicity, their impact on the anticancer efficacy of the carrier-mediated drug is unclear. Macrophages play a central role in clearance of nanoparticles from the circulation but the impact of the nanoparticles on the functionality of macrophages remains to be fully elucidated.

Our findings reveal that macrophages mediate the protumoral effects of PLN through immunosuppressive mechanisms as indicated by polarization of tumor macrophages towards a mixed M1/M2-phenotype and increased arginase-expressing immature myeloid-derived cells. Mechanistically, PLNs that are phagocytosed by myeloid cells may activate an anti-inflammatory program much like that associated with uptake of apoptotic cells [48, 49] that would spur TGFβ production by macrophages. In fact, uptake of liposomes by peritoneal macrophage can induce a tolerogenic M2-like phenotype [50]. The production of TGFβ by these tolerogenic myeloid cells can lead to secondary release of C-C motif chemokine ligand 2 (CCL2, also known as monocyte chemotactic protein 1 [MCP-1]) and emigration of immature myeloid cells from the bone marrow into circulation and organs of the MPS such as spleen [51, 52] (Figure 8). Consistent with this hypothesis, we found increased splenic infiltration of immature myeloid cell populations such as inflammatory monocytes that have the potential to differentiate into both M1 and M2 macrophages [53, 54]. Based on the inflammatory state of an organ, immature myeloid cells may then take on anti-inflammatory properties associated with M2 activation that impair T-cell mediated immunity [55], increase neoangiogenesis [56, 57], and spur tumor growth (Figure 8). Indeed, our results show that PLN treatment was associated with global suppression of cytokine production in tumor infiltrating T-cells. Moreover, recent evidence in patients with ovarian cancer showed that circulating monocyte numbers and plasma CCL2 levels correlated with PLD clearance [23] and plasma PLD levels [58], respectively. In addition, CCL2 knockout mice bearing ovarian tumor xenografts were found to have altered clearance of PLD as compared to control mice [58, 59]. These data further support a link between PLN uptake by myeloid cells of the monocyte-macrophage lineage and their immune functionality.

Figure 8. Proposed mechanisms of PLN-induced tumor growth and immunosuppression. A: Liposomes penetrate and deposit in the tumor via enhanced permeability and retention (EPR) effect; B: Tumor-associated macrophages phagocytose liposomes, and respond with increased arginase production, decrease iNOS, and shift toward an M2 phenotype; C: An autocrine/paracrine loop of TGFβ ensues and leads to secretion of CCL2 (MCP-1); D: CCL2 attracts peripheral migration of immature myeloid cells which increase arginase production and turn into suppressive cells; E: TAM and myeloid-derived suppressor cells (MDSC) impair T-cell immunity; F: Cytotoxic T lymphocyte (CTL) antitumor effects are inhibited.

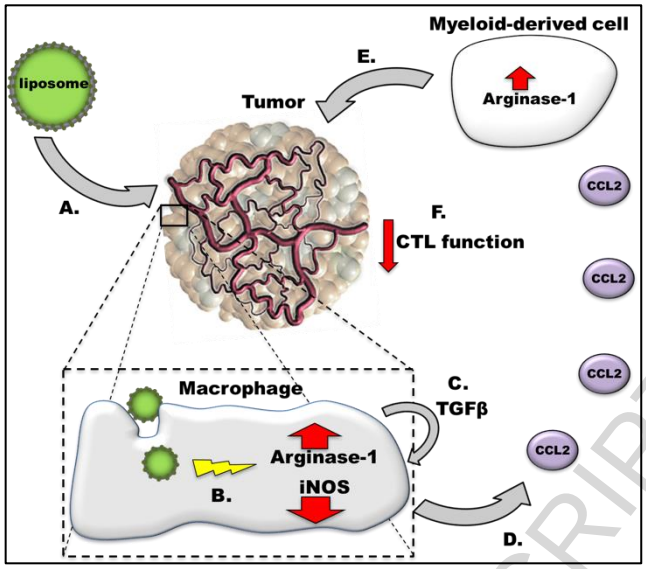

The extent to which our findings are broadly applicable to other nanoparticles remains to be determined. There is substantial heterogeneity in physical (e.g., size, shape, charge) and chemical (e.g., composition) properties among different types of nanomedicines, and these physicochemical parameters are known to affect their *in vivo* pharmacokinetics and pharmacodynamics. Hence, it should not be assumed that our observations will be generalizable beyond the PLN that we tested. Further studies are also warranted to identify the PLN component that is responsible for immunomodulation and elucidate the precise molecular mechanisms. There is strong evidence in the literature for PEG as an agent in reducing immunogenicity and as an immunosuppressive-camouflage agent [60, 61]. In cancer drug delivery, PEG-lipid nanoemulsions (mean particle size 125 nm) induced immunologic tolerance that was mediated by macrophages [62]. In protein therapeutics, PEG suppressed antibody responses against conjugated antigens thereby inducing a tolerogenic state [63] and this approach has been utilized to optimize pharmacokinetics of therapeutic proteins (e.g. PEG-asparaginase) [64]. In organ transplantation, the addition of PEG to organ preservation solutions significantly improved organ function and decreased inflammation and fibrosis through suppression of the host immune responses against the transplanted organ [65, 66]. The immune modulatory effects of PEG are increasingly recognized, and the use of PEG in cancer drug delivery has become a controversy [67] that is unlikely to be resolved until the precise mechanisms, and its impact on anticancer efficacy of the payload drug, are clarified.

Even if PEG is the moiety responsible for immunosuppression, it may not be possible to forgo the use of PEG in all nanomedicines. Pegylation has been a successful strategy to prolong the circulating half-life of liposome-delivered drugs and this has directly correlated with enhanced tumor drug accumulation. Moreover, given that there are several PLN-drugs already approved for use in patients, it would be imperative to identify strategies to mitigate the undesired immunosuppression induced by the PLN carrier [68, 69]. Importantly, we demonstrated here that PLN-alen, but not free alendronate, mitigated the tumor-promoting effects of the PLN carrier. Encapsulating alendronate into PLN reversed carrier-associated effects on myeloid cell functionality and accumulation in tumor and spleen. Given that PLN-alen hardly interacts with tumor cells *in vitro* and has not been found to have direct cytotoxicity on numerous tumorigenic cell lines (IC_{50} values greater than 50 μM, unpublished data from the Gabizon laboratory and from the National Cancer Institute's Nanotechnology Characterization Laboratory), the observed inhibition of tumor growth is likely due to the immune modulatory effects of PLN-alen.

Aminobisphosphonates, such as alendronate, are potent inhibitors of the mevalonate pathway which is being targeted as a strategy to promote immunogenic destruction of cancer cells [26]. Aminobisphosphonates have been shown to have immune stimulatory effects such as induction of proinflammatory cytokines, sensitization of macrophages to inflammatory stimuli, and activation of gamma-delta T-cells [70]. In contrast, non-aminobisphosphonates such as clodronate, primarily act via production of toxic ATP analogues and have been shown to inhibit production of inflammatory mediators and cause overall macrophage suppression and toxicity [70, 71]. Encapsulation of alendronate into liposomes is likely to modify the immune modulatory effects of the drug, as the carrier will dictate the pharmacokinetic profile and may drastically alter cellular and molecular interactions. The fact that PLN-alen potentiated $IFN\gamma^{+}perforin^{+}$ responses in multi-cytokine producing T-cells (Supplemental Figure S4) suggests increased T-cell cytolytic potential that may partially explain the moderate antitumor activity we observed with PLN-alen treatment. It is likely that there are additional immunomodulatory effects of PLN-alen on other cell types such as gamma-delta T-cells [25] that will need to be fully elucidated and may be relevant particularly in humans. Together, these data suggest the co-encapsulation of aminobisphosphonates with other immunotherapies or chemotherapies as one possible strategy to significantly enhance the anticancer efficacy of liposome-mediated drugs. This approach is strongly supported by a recent report by Shmeeda, et al. that co-encapsulating alendronate with doxorubicin in a PLN resulted in synergistic anticancer activity in an immunocompetent mouse model of cancer [30]. Interestingly, there was no synergy observed in an immunodeficient tumor model [30], which is consistent with the immunomodulatory mechanisms of action of alendronate that we and others [25] have observed.

The extent to which our findings are generalizable to other types of tumors remains to be determined. While we observed in the TC-1 tumor model that the impact of PLN and PLN-alen was greatest for mixed M1/M2 TAMs, others have reported that liposomal aminobisphosphonates increased M1 polarization of J774 murine macrophages when co-cultured with 4T1 breast cancer cells ([72]. There are several factors that may explain these disparate observations including differences in tumor biology, differences in functionality of primary TAMs versus immortal macrophage cell lines, and differences between *in vitro* versus *in vivo* exposure to liposomes. Given that there is significant heterogeneity in tumor immunogenicity and response to therapeutic interventions between different types of malignancies, additional studies are warranted to identify the tumor parameters that determine responses to nanomedicines and to delineate the mechanisms involved.

Our findings challenge the current dogma that PLNs are inert drug carriers, and we theorize that the immunosuppressive properties of PLN have previously been overlooked for several reasons. First, the doses of PLN anticancer drugs used in animal models is typically much larger than that used in patients, which may allow the drug cargo effects to override the immunosuppressive effect of the carrier. This may explain why nanomedicines clearly outperform the free drug comparator in preclinical studies while the differences are very small in clinical trials. In addition, preclinical drug development strategies have historically focused on antiproliferative effects of the drug payload, and not on evaluating immune modulatory or protumoral effects of the PLN carrier. Hence, tumor models were selected that are highly sensitive to cytotoxic effects of PLN-drugs, but these models were not sensitive to protumoral effects and their immune-responsiveness is not well characterized. Moreover, the desire to evaluate tumoricidal effects in human cancer cells also led to the prevalent use of immune deficient mouse models that likely contributed to the masking of immunosuppressive effects of PLNs. Even among the immunocompetent mouse models, there are major differences in global immune status (e.g., balance of Th1-Th2 cytokines or M1-M2 macrophages) [73] that affect nanoparticle disposition.

The Th1-dominant strains such as C57BL/6 were reported to have slower rates of clearance of pegylated 300-nm cylindrical hydrogel nanoparticles than the Th2-dominant strains such as BALB/c [74]. These differences in clearance were correlated with M1 macrophage polarization and lower particle uptake in Th1 strains, and M2 macrophage polarization and higher nanoparticle uptake in the Th2 strains. Likewise, when silica nanoparticles were tested *in vitro* with THP1 cells, an immortalized human monocytic cell line, alternatively activated (M2-like) THP1 cells demonstrated higher nanoparticle uptake than classically activated (M1-like) THP1 cells [75].

We believe that the dearth of *in vivo* and long-term immunological studies during the preclinical development of nanoparticle drugs [76] contributed to missing the immunosuppressive properties of some nanoparticles such as PLN. The preclinical evaluation of the immunological effects of nanoparticles have historically relied on *in vitro* studies and short-term studies in animal models which are best suited for evaluating acute effects such as induction of blood complement activation and cytokine release syndromes. Whereas, immunosuppressive effects, especially those that affect the adaptive immune system, tend to manifest after longer periods and require more complex *in vivo* immunological assessments such as the ones that we conducted in this study. Given the pivotal roles of the immune system in both cancer progression and regression, we propose that immune-responsive tumor models and in-depth immune functional studies should be incorporated in the current preclinical drug development paradigm for cancer nanomedicines.

5.0 Conclusion

Liposomes will likely continue to be heavily utilized for cancer drug delivery since they have been the most successful clinically and are proven to improve drug tolerability in cancer patients. While nanoparticle drug delivery has the potential to also significantly improve anticancer efficacy, these expectations remain to be broadly realized in the clinic for the treatment of solid tumors. We have begun to identify some of the barriers to clinical translation and unravel the mechanisms of interactions between PLNs and the immune system. We anticipate that this work will lay the foundation for the development of new preclinical models with increased clinical relevance and new therapeutic approaches targeting macrophage functional polarization to enhance the anticancer efficacy of PLN drugs. Importantly, we show that PLN-alendronate can reverse the effects of the PLN carrier on macrophages, supporting combination therapy with liposomal alendronate as a rapidly translatable strategy to increase the anticancer efficacy of liposomal drugs since alendronate is already approved for treatment of osteoporosis. As with traditional cytotoxic chemotherapy, the next generation of immunotherapies will also likely strive to exploit nanoparticle drug delivery as a strategy to increase tumor specificity and improve pharmacokinetic parameters. It is therefore imperative that the complex interactions between the drug cargo, carrier, and tumor immunologic milieu are well understood and utilized to achieve the full anticancer potential of carrier-mediated therapies [11].

Acknowledgements

We would like to thank Ms. Jenny Gorin, Ms. Rebecca Stark, and Ms. Min (Bella) Xie for their technical assistance with liposome preparation/characterization, cell culture studies, and supplemental qPCR studies, respectively.

References

1. Nakanishi W, Minami K, Shrestha LK et al. Bioactive nanocarbon assemblies: Nanoarchitectonics and applications. NanoToday 2014; 9: 378-394.
2. Hare JI, Lammers T, Ashford MB et al. Challenges and strategies in anti-cancer nanomedicine development: An industry perspective. Adv Drug Deliv Rev 2017; 108: 25-38.
3. Allen TM, Cullis PR. Liposomal drug delivery systems: from concept to clinical applications. Adv Drug Deliv Rev 2013; 65: 36-48.
4. Papahadjopoulos D, Allen TM, Gabizon A et al. Sterically stabilized liposomes: improvements in pharmacokinetics and antitumor therapeutic efficacy. Proc Natl Acad Sci U S A 1991; 88: 11460-11464.
5. Gabizon AA, Patil Y, La-Beck NM. New insights and evolving role of pegylated liposomal doxorubicin in cancer therapy. Drug Resist Updat 2016; 29: 90-106.
6. Gordon AN, Fleagle JT, Guthrie D et al. Recurrent epithelial ovarian carcinoma: a randomized phase III study of pegylated liposomal doxorubicin versus topotecan. J Clin Oncol 2001; 19: 3312-3322.
7. O'Brien ME, Wigler N, Inbar M et al. Reduced cardiotoxicity and comparable efficacy in a phase III trial of pegylated liposomal doxorubicin HCl (CAELYX/Doxil) versus conventional doxorubicin for first-line treatment of metastatic breast cancer. Ann Oncol 2004; 15: 440-449.
8. Gibson JM, Alzghari S, Ahn C et al. The role of pegylated liposomal doxorubicin in ovarian cancer: a meta-analysis of randomized clinical trials. Oncologist 2013; 18: 1022-1031.
9. Petersen GH, Alzghari SK, Chee W et al. Meta-analysis of clinical and preclinical studies comparing the anticancer efficacy of liposomal versus conventional non-liposomal doxorubicin. J Control Release 2016; 232: 255-264.
10. Lammers T, Kiessling F, Hennink WE, Storm G. Drug targeting to tumors: principles, pitfalls and (pre-) clinical progress. J Control Release 2012; 161: 175-187.
11. Anchordoquy TJ, Barenholz Y, Boraschi D et al. Mechanisms and Barriers in Cancer Nanomedicine: Addressing Challenges, Looking for Solutions. ACS Nano 2017; 11: 12-18.
12. Lancet JE, Uy GL, Cortes JE et al. Final results of a phase III randomized trial of CPX-351 versus 7+3 in older patients with newly diagnosed high risk (secondary) AML. Journal of Clinical Oncology 2016; 34: 7000-7000.
13. Zarour HM. Reversing T-cell Dysfunction and Exhaustion in Cancer. Clin Cancer Res 2016; 22: 1856-1864.
14. Beatty GL, Gladney WL. Immune escape mechanisms as a guide for cancer immunotherapy. Clin Cancer Res 2015; 21: 687-692.
15. Chang AL, Miska J, Wainwright DA et al. CCL2 Produced by the Glioma Microenvironment Is Essential for the Recruitment of Regulatory T Cells and Myeloid-Derived Suppressor Cells. Cancer Res 2016; 76: 5671-5682.
16. Mantovani A, Sozzani S, Locati M et al. Macrophage polarization: tumor-associated macrophages as a paradigm for polarized M2 mononuclear phagocytes. Trends Immunol 2002; 23: 549-555.
17. Gabrilovich DI, Nagaraj S. Myeloid-derived suppressor cells as regulators of the immune system. Nat Rev Immunol 2009; 9: 162-174.
18. La-Beck NM, Gabizon AA. Nanoparticle Interactions with the Immune System: Clinical Implications for Liposome-Based Cancer Chemotherapy. Front Immunol 2017; 8: 416.
19. Moghimi SM. Cancer nanomedicine and the complement system activation paradigm: anaphylaxis and tumour growth. J Control Release 2014; 190: 556-562.
20. Sabnani MK, Rajan R, Rowland B et al. Liposome promotion of tumor growth is associated with angiogenesis and inhibition of antitumor immune responses. Nanomedicine 2015; 11: 259-262.
21. Markman M, Gordon AN, McGuire WP, Muggia FM. Liposomal anthracycline treatment for ovarian cancer. Semin Oncol 2004; 31: 91-105.
22. Caron WP, Lay JC, Fong AM et al. Translational studies of phenotypic probes for the mononuclear phagocyte system and liposomal pharmacology. J Pharmacol Exp Ther 2013; 347: 599-606.
23. La-Beck NM, Zamboni BA, Gabizon A et al. Factors affecting the pharmacokinetics of pegylated liposomal doxorubicin in patients. Cancer Chemother Pharmacol 2012; 69: 43-50.

24. Mantovani A, Bottazzi B, Colotta F et al. The origin and function of tumor-associated macrophages. Immunol Today 1992; 13: 265-270.
25. Parente-Pereira AC, Shmeeda H, Whilding LM et al. Adoptive immunotherapy of epithelial ovarian cancer with Vgamma9Vdelta2 T cells, potentiated by liposomal alendronic acid. J Immunol 2014; 193: 5557-5566.
26. Riganti C, Massaia M. Inhibition of the mevalonate pathway to override chemoresistance and promote the immunogenic demise of cancer cells: Killing two birds with one stone. Oncoimmunology 2013; 2: e25770.
27. Lin KY, Guarnieri FG, Staveley-O'Carroll KF et al. Treatment of established tumors with a novel vaccine that enhances major histocompatibility class II presentation of tumor antigen. Cancer Res 1996; 56: 21-26.
28. Ji H, Chang EY, Lin KY et al. Antigen-specific immunotherapy for murine lung metastatic tumors expressing human papillomavirus type 16 E7 oncoprotein. Int J Cancer 1998; 78: 41-45.
29. Gabizon A, Papahadjopoulos D. The role of surface charge and hydrophilic groups on liposome clearance in vivo. Biochim Biophys Acta 1992; 1103: 94-100.
30. Shmeeda H, Amitay Y, Gorin J et al. Coencapsulation of alendronate and doxorubicin in pegylated liposomes: a novel formulation for chemoimmunotherapy of cancer. J Drug Target 2016; 24: 878-889.
31. Burnett SH, Kershen EJ, Zhang J et al. Conditional macrophage ablation in transgenic mice expressing a Fas-based suicide gene. J Leukoc Biol 2004; 75: 612-623.
32. Morris SM, Jr., Kepka-Lenhart D, Chen LC. Differential regulation of arginases and inducible nitric oxide synthase in murine macrophage cells. Am J Physiol 1998; 275: E740-747.
33. Gordon S. Alternative activation of macrophages. Nat Rev Immunol 2003; 3: 23-35.
34. Mansouri H. Simultaneous inference based on rank statistics in linear models. Journal of Statistical Computation and Simulation 2015; 85: 660-674.
35. Mansouri H. Multifactor Analysis of Variance Based on the Aligned Rank Transform Technique. Computational Statistics and Data Analysis 1999; 29: 177-189.
36. Bronte V, Pittet MJ. The spleen in local and systemic regulation of immunity. Immunity 2013; 39: 806-818.
37. Fotiadis C, Zografos G, Aronis K et al. The effect of various types of splenectomy on the development of B-16 melanoma in mice. Anticancer Res 1999; 19: 4235-4239.
38. Pobezinskii LA, Pobezinskaya EL, Zvezdova ES et al. Accumulation of neutrophils in the spleen of mice immunized with cells of allogenic tumors. Dokl Biol Sci 2005; 402: 224-229.
39. Kusmartsev SA, Li Y, Chen SH. Gr-1+ myeloid cells derived from tumor-bearing mice inhibit primary T cell activation induced through CD3/CD28 costimulation. J Immunol 2000; 165: 779-785.
40. Pillay J, Tak T, Kamp VM, Koenderman L. Immune suppression by neutrophils and granulocytic myeloid-derived suppressor cells: similarities and differences. Cell Mol Life Sci 2013; 70: 3813-3827.
41. Caron WP, Song G, Kumar P et al. Interpatient pharmacokinetic and pharmacodynamic variability of carrier-mediated anticancer agents. Clin Pharmacol Ther 2012; 91: 802-812.
42. Song G, Petschauer JS, Madden AJ, Zamboni WC. Nanoparticles and the mononuclear phagocyte system: pharmacokinetics and applications for inflammatory diseases. Curr Rheumatol Rev 2014; 10: 22-34.
43. Chanan-Khan A, Szebeni J, Savay S et al. Complement activation following first exposure to pegylated liposomal doxorubicin (Doxil): possible role in hypersensitivity reactions. Ann Oncol 2003; 14: 1430-1437.
44. Szebeni J, Muggia F, Gabizon A, Barenholz Y. Activation of complement by therapeutic liposomes and other lipid excipient-based therapeutic products: prediction and prevention. Adv Drug Deliv Rev 2011; 63: 1020-1030.
45. Szebeni J, Baranyi L, Savay S et al. Liposome-induced pulmonary hypertension: properties and mechanism of a complement-mediated pseudoallergic reaction. Am J Physiol Heart Circ Physiol 2000; 279: H1319-1328.
46. Harrington KJ, Mohammadtaghi S, Uster PS et al. Effective targeting of solid tumors in patients with locally advanced cancers by radiolabeled pegylated liposomes. Clin Cancer Res 2001; 7: 243-254.
47. Weinstock SB, Brain JD. Comparison of particle clearance and macrophage phagosomal motion in liver and lungs of rats. J Appl Physiol (1985) 1988; 65: 1811-1820.

48. Freire-de-Lima CG, Nascimento DO, Soares MB et al. Uptake of apoptotic cells drives the growth of a pathogenic trypanosome in macrophages. Nature 2000; 403: 199-203.
49. N AG, Bensinger SJ, Hong C et al. Apoptotic cells promote their own clearance and immune tolerance through activation of the nuclear receptor LXR. Immunity 2009; 31: 245-258.
50. Cruz-Leal Y, Lucatelli Laurindo MF, Osugui L et al. Liposomes of phosphatidylcholine and cholesterol induce an M2-like macrophage phenotype reprogrammable to M1 pattern with the involvement of B-1 cells. Immunobiology 2014; 219: 403-415.
51. Smythies LE, Maheshwari A, Clements R et al. Mucosal IL-8 and TGF-beta recruit blood monocytes: evidence for cross-talk between the lamina propria stroma and myeloid cells. J Leukoc Biol 2006; 80: 492-499.
52. Zhang F, Tsai S, Kato K et al. Transforming growth factor-beta promotes recruitment of bone marrow cells and bone marrow-derived mesenchymal stem cells through stimulation of MCP-1 production in vascular smooth muscle cells. J Biol Chem 2009; 284: 17564-17574.
53. Arnold L, Henry A, Poron F et al. Inflammatory monocytes recruited after skeletal muscle injury switch into antiinflammatory macrophages to support myogenesis. J Exp Med 2007; 204: 1057-1069.
54. Gallina G, Dolcetti L, Serafini P et al. Tumors induce a subset of inflammatory monocytes with immunosuppressive activity on CD8+ T cells. J Clin Invest 2006; 116: 2777-2790.
55. Van Ginderachter JA, Meerschaut S, Liu Y et al. Peroxisome proliferator-activated receptor gamma (PPARgamma) ligands reverse CTL suppression by alternatively activated (M2) macrophages in cancer. Blood 2006; 108: 525-535.
56. Zajac E, Schweighofer B, Kupriyanova TA et al. Angiogenic capacity of M1- and M2-polarized macrophages is determined by the levels of TIMP-1 complexed with their secreted proMMP-9. Blood 2013; 122: 4054-4067.
57. Jetten N, Verbruggen S, Gijbels MJ et al. Anti-inflammatory M2, but not pro-inflammatory M1 macrophages promote angiogenesis in vivo. Angiogenesis 2014; 17: 109-118.
58. Song G, Tarrant TK, White TF et al. Roles of chemokines CCL2 and CCL5 in the pharmacokinetics of PEGylated liposomal doxorubicin in vivo and in patients with recurrent epithelial ovarian cancer. Nanomedicine 2015; 11: 1797-1807.
59. Song G, Darr DB, Santos CM et al. Effects of tumor microenvironment heterogeneity on nanoparticle disposition and efficacy in breast cancer tumor models. Clin Cancer Res 2014; 20: 6083-6095.
60. Veronese FM, Mero A. The impact of PEGylation on biological therapies. BioDrugs 2008; 22: 315-329.
61. Chen AM, Scott MD. Current and future applications of immunological attenuation via pegylation of cells and tissue. BioDrugs 2001; 15: 833-847.
62. Wang L, Wang C, Jiao J et al. Tolerance-like innate immunity and spleen injury: a novel discovery via the weekly administrations and consecutive injections of PEGylated emulsions. Int J Nanomedicine 2014; 9: 3645-3657.
63. Sehon AH. Carl Prausnitz Memorial Lecture. Suppression of antibody responses by chemically modified antigens. Int Arch Allergy Appl Immunol 1991; 94: 11-20.
64. Fu CH, Sakamoto KM. PEG-asparaginase. Expert Opin Pharmacother 2007; 8: 1977-1984.
65. Hauet T, Eugene M. A new approach in organ preservation: potential role of new polymers. Kidney Int 2008; 74: 998-1003.
66. Tokunaga Y, Wicomb WN, Garcia-Kennedy R et al. The immunosuppressive effect of polyethylene glycol in a flush solution for rat liver transplantation. Transplantation 1992; 54: 756-758.
67. Verhoef JJ, Anchordoquy TJ. Questioning the Use of PEGylation for Drug Delivery. Drug Deliv Transl Res 2013; 3: 499-503.
68. Moghimi SM, Hunter AC, Andresen TL. Factors controlling nanoparticle pharmacokinetics: an integrated analysis and perspective. Annu Rev Pharmacol Toxicol 2012; 52: 481-503.
69. Abu Lila AS, Eldin NE, Ichihara M et al. Multiple administration of PEG-coated liposomal oxaliplatin enhances its therapeutic efficacy: a possible mechanism and the potential for clinical application. Int J Pharm 2012; 438: 176-183.

70. Santini D, Fratto ME, Vincenzi B et al. Bisphosphonate effects in cancer and inflammatory diseases: in vitro and in vivo modulation of cytokine activities. BioDrugs 2004; 18: 269-278.
71. Frith JC, Monkkonen J, Blackburn GM et al. Clodronate and liposome -encapsulated clodronate are metabolized to a toxic ATP analog, adenosine 5'-(beta, gamma-dichloromethylene) triphosphate, by mammalian cells in vitro. J Bone Miner Res 1997; 12: 1358-1367.
72. Sousa S, Auriola S, Monkkonen J, Maatta J. Liposome encapsulated zoledronate favours M1-like behaviour in murine macrophages cultured with soluble factors from breast cancer cells. BMC Cancer 2015; 15: 4.
73. Watanabe H, Numata K, Ito T et al. Innate immune response in Th1- and Th2-dominant mouse strains. Shock 2004; 22: 460-466.
74. Jones SW, Roberts RA, Robbins GR et al. Nanoparticle clearance is governed by Th1/Th2 immunity and strain background. J Clin Invest 2013; 123: 3061-3073.
75. Hoppstadter J, Seif M, Dembek A et al. M2 polarization enhances silica nanoparticle uptake by macrophages. Front Pharmacol 2015; 6: 55.
76. Ilinskaya AN, Dobrovolskaia MA. Immunosuppressive and anti-inflammatory properties of engineered nanomaterials. Br J Pharmacol 2014; 171: 3988-4000.

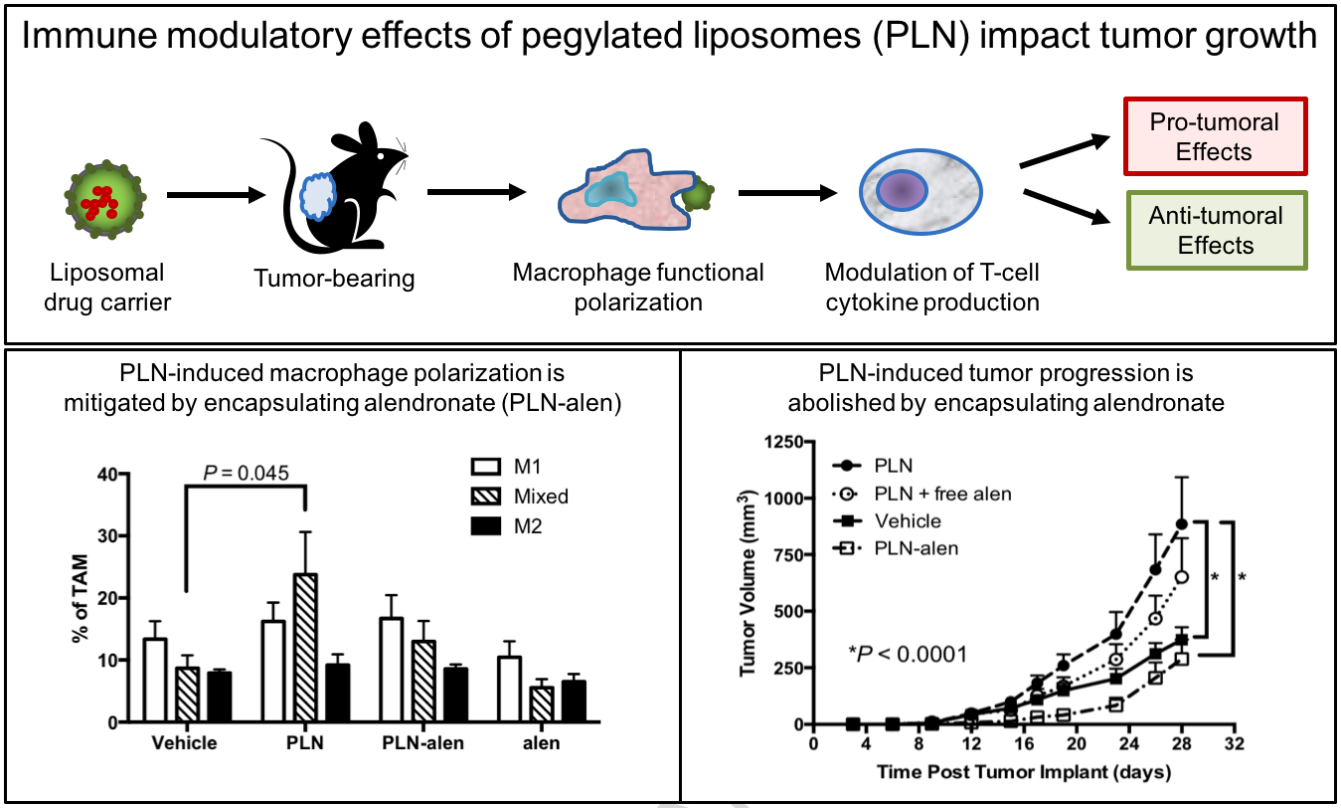

Graphical abstract